Spring 5-1-2015

Oscillatory Activity in the Subthalamic Nucleus and Motor Cortex in a Pharmacological Model of Parkinsonian Tremor

Aileen F. Haque
University of Connecticut - Storrs, aileenhaque@gmail.com

Oscillatory Activity in the Subthalamic Nucleus and Motor Cortex In A Pharmacological Rodent Model of Parkinsonian Tremor

The Honors Scholar Thesis of
Aileen Haque

Advisor: Dr. John Salamone
University of Connecticut, Storrs, CT 06269
May 2015

Acknowledgements

First, I would like to thank my honors thesis advisor Professor John D. Salamone for his support and mentorship throughout my undergraduate experience. I value is input and patience in helping me understand the many aspects of behavioral neuroscience and being a resource to me whenever needed. This experience has helped me grow both academically and personally. I could not have asked for a better, more knowledgeable advisor.

Next, I would like to thank Samantha Podurgiel for her mentorship in this project and teaching me necessary skills for this project. She has been wonderful throughout this experience and provided guidance at every step of the way in this project. I am grateful for her assistance in my research endeavors and give my sincere thanks for the time and commitment she has devoted to my learning process.

I would also like to thank Samantha Yohn for the hours spent teaching me laboratory techniques during my years spent in the Salamone lab and her helpful guidance. I am grateful to her for her assistance in my research endeavors and give her my sincere thanks for the time and commitment she devoted to my learning process.

Additionally, I would also like to thank Lauren Long, Emily Errante, and James Chrobak for their contributions to the study. This work was supported by a SURF grant and Honors Life Sciences Thesis Award grant for the UConn Office of Undergraduate Research.

Abstract

Parkinson's Disease (PD) is a motor disorder with symptoms including resting tremor, akinesia, bradykinesia, and rigidity. A major neuropathological feature of PD is degeneration of nigrostriatal dopamine (DA) neurons. The resulting DA depletions lead to the production of severe motor deficits. Pharmacological agents that reduce DA transmission can also induce these motor abnormalities. In addition to the involvement of DA, drugs acting on acetylcholine, namely cholinomimetics, can induce or exacerbate Parkinsonian symptoms. In humans, one of the main motor symptoms associated with PD is resting tremor, occurring at a frequency of 3-7 Hz. This can be modeled in rodents using a tremulous jaw movement (TJM) model; these movements are defined as rapid, repetitive, vertical deflections of the lower jaw that are not directed at any particular stimulus. In rodents, TJMs are induced using the same pharmacological agents that induce Parkinsonism in humans, including neurotoxic or pharmacological depletion of striatal dopamine, dopamine depleting agents, such as tetrabenazine (TBZ), dopamine antagonists, and cholinomimetics, such as pilocarpine. Moreover, TJMs in rodents can be attenuated by antiparkinsonian agents, including L-DOPA, dopamine agonists, muscarinic antagonists, and adenosine A_{2A} antagonists. In human Parkinsonian patients, exaggerated physiological synchrony is seen in the beta frequency band in various parts of the cortical/basal ganglia/thalamic circuitry, and activity in the tremor frequency range (3-7 Hz) also has been recorded. In past studies, local field potentials (LFPs) have been recorded from PD patients undergoing implantation of stimulating electrodes in the subthalamic nucleus (STN). It has been shown that there is a high degree of coherence between STN LFPs and tremor as measured by EMG in PD patients. This study was done to determine if tremor-related local field potential (LFP) activity could be recorded from motor cortex or subthalamic nucleus during the TJMs

induced by the muscarinic agonist pilocarpine, which is a well-known tremorogenic agent. Pilocarpine induced a robust TJM response that was marked by rhythmic electromyographic activity in the temporalis muscle. Compared to periods with no tremor activity, TJM epochs were characterized by increased LFP activity in the tremor frequency range in both neocortex and subthalamic nucleus. Tremor activity was not associated with increased activity in the beta frequency band. These studies identified tremor-related LFP activity in parts of the cortical/basal ganglia circuitry that are involved in the pathophysiology of Parkinsonism, which may ultimately lead to identification of the oscillatory neural mechanisms involved in the generation of tremulous activity, as well as novel treatments for tremor disorders.

1. Introduction

Parkinsonism is a broad family of motor movement disorders that includes idiopathic Parkinson's disease (PD) and drug-induced Parkinsonism (DIP), as well as pugilistic and post-encephalic Parkinsonism. PD results from the death of dopamine (DA) producing cell bodies in the Substantia Nigra Pars Compacta, causing a degeneration of nigrostriatal DA neurons (Hornykiewicz, 1973), It is progressive neurodegenerative disease that will affect muscles throughout the entire body and can lead to a decrease in cognitive skills over many years. There are millions of cases known worldwide, with 1-2 million diagnosed in the United States. PD is the second most common neurodegenerative known disorder, with a prevalence of 1-2% in people over age 65 and 3% prevalence in those over age 85. Age is the strongest risk factor for PD and given the aging of the population, prevalence is expected to increase dramatically over the next decade.

DIP is induced by drugs that interfere with DA transmission (e.g. DA antagonists, DA depleting agents; Marsden et al., 1975; McEvoy, 1983), and cholinomimetics such as anticholinesterases and muscarinic agonists (Ott and Lannon, 1992; Aarsland et al., 2003). The cardinal motor symptoms of Parkinsonism include akinesia, bradykinesia, rigidity, and resting tremor, which typically occurs in the 3-7 Hz frequency range (Marsden et al., 1975). Parkinsonian symptoms including tremor are produced by a cascade of neurochemical and physiological events involving transmitters in various parts of basal ganglia circuitry (Salamone et al. 1998).

In addition to the involvement of DA, drugs acting on acetylcholine (cholinomimetics) also can induce or exacerbate Parkinsonian symptoms, including tremor, in humans, and muscarinic acetylcholine antagonists often are used as antiparkinsonian agents that can suppress tremor. Tremor is defined as a "periodic oscillation of a body member" (Findley and Gresty, 1981), and can be a feature of several different movement disorders. Tremors are classified in various ways, including the state under which they occur (e.g., resting tremor, action tremor), their local frequency, and pathological conditions associated with tremor.

Relatively few clinical studies have specifically emphasized the pharmacology of tremor, and there is considerable uncertainty about the neurochemical mechanisms that underlie tremorogenesis (Deuschl et al. 2000). For these reasons, it is important to focus attention on the pharmacology, neurochemistry, and physiology of tremor, and studies employing animal models are a critical aspect of this research strategy. Drug-induced tremulous jaw movements are a model of Parkinsonian tremor (Salamone et al. 1998, 2005). DIP is produced in rodents by the same pharmacological agents that induce human Parkinsonism, and resting tremor can be modeled in rodents using the tremulous jaw movement (TJM) model. TJMs are defined as

"rapid, repetitive vertical deflections of the lower jaw that resemble chewing but are not directed at any particular stimulus", and this model has become an extensively validated model of Parkinsonian resting tremor in rodents (Salamone et al. 1998). TJMs occur in phasic bursts of activity in the 3-7 Hz local frequency range, which resembles the frequency of Parkinsonian resting tremor (Salamone et al., 1998; Cousins et al., 1998; Collins et al., 2010; Podurgiel et al., 2013b).

More recently, there has been substantial interest in DA/adenosine receptor interactions, as adenosine A_{2A} receptors are highly expressed in neostriatum. A_{2A} antagonists exert motor effects in rodents and primates that are consistent with antiparkinsonian actions, including suppression of TJMs (Correa et al. 2004; Salamone et al. 2008). TJMs in rats can be induced by several DAergic conditions that are known to be associated with Parkinsonism in humans, including neurotoxic depletion of striatal DA (Jicha and Salamone, 1991), reserpine (Baskin and Salamone, 1993; Salamone and Baskin, 1996; Salamone et al. 2008), and DA antagonists (i.e., Jicha and Salamone, 1991). TJMs can also be induced by muscarinic agonists (Salamone et al. 1986; Salamone et al. 1990) and anticholinesterases such as physostigmine, tacrine or galantamine (Mayorga et al. 1997). TJMs can be attenuated by co-administration of antiparkinsonian drugs from several different classes, such as L-DOPA, DA agonists, muscarinic antagonists, MAO inhibitors, and adenosine A2A antagonists (Cousins et al., 1997; Simola et al., 2004, 2006; Salamone et al., 2005, 2008a,b; Podurgiel et al., 2013a,b). Considerable evidence indicates that TJMs in rodents are a valid model for the exploration of the pharmacology, neurochemistry and physiology of drug-induced tremor (Salamone et al., 1998, 2008b, 2013; Collins-Praino et al., 2011; Podurgiel et al., 2013a,b, 2015). Furthermore, TJMs can be

attenuated by deep brain stimulation of the subthalamic nucleus (Collins-Praino et al. 2012), which is a major brain target in human deep brain stimulation Parkinsonism treatments.

There have been physiological measurements of oscillatory activity in the basal ganglia circuits and cortex in humans with PD as well as in animal models. The best characterized oscillation depicting the exaggerated neuronal synchrony found in the basal ganglia and cortex of PD patients is the beta band, which is at about 15-30 Hz (Brown 2003; Hammond et al., 2007; Oswal et al., 2013). Increased beta activity has been observed within the cortex (George et al., 2013) and subthalamic nucleus (STN) of PD patients, and it has been suggested that exclusive synchrony in this frequency range contributes to motor dysfunction (Levy et al., 2002; Brown and Williams, 2005; Kuhn et al., 2006). This has been demonstrated in terms of increases in oscillatory activity in the discharge of single neurons, increased amplitude of local field potentials (LFPs), and increased coherence of LFP signals across different basal ganglia structures in patients undergoing surgical procedures (Hutchison et al., 2004; Hammond et al., 2007). LFPs reflect synchronous synaptic input onto the somatodendritic field of multiple adjacent neurons (Creutzfeldt et al., 1966). Thus, an increase in the amplitude or change in frequency of the LFP can reflect increasing synchrony among a population of input neurons, or a change in the frequency of a population input (see Buzsaki and Chrobak, 1995). Increases in synchrony result from increased periodic discharge of individual neurons, or more typically from altered temporal organization of a group of neurons, in which any one neuron may or may not be oscillatory, but the population exhibits a repeating (oscillatory) temporal structure (see Buzsaki and Chrobak, 1995).

Reduction in STN beta activity correlates with improvement in akinesia and rigidity in PD patients (Levy et al., 2002; Kuhn et al., 2006). While the literature supports a link between increased cortical and basal ganglia beta power and the development of akinesia/rigidity, beta

activity generally does not correlate with the severity of resting tremor (Kuhn et al., 2005; Hammond et al., 2007; Oswal et al., 2013). Rather, the development of tremor in PD patients has been shown to be associated with the emergence of oscillations in the tremor frequency range (3-7 Hz) in the cortex and basal ganglia (Timmerman et al., 2003; Reck et al., 2009; Hirschmann et al., 2013; Oswal et al., 2013). Timmerman et al. (2003) reported strong coherence between electromyograph (EMG) activity of forearm muscles and activity in the contralateral primary motor cortex (M1), at tremor (3-7 Hz) and double tremor frequency (7-13 Hz) in PD patients off medication. Similar patterns of activity have been observed in the STN of PD patients, as indicated by power spectra peaks at tremor frequency and tremor harmonics, as well as significant coherence between STN LFPs and EMG activity at tremor frequency (Brown et al., 2001; Levy et al., 2000; Liu et al., 2002; Wang et al., 2005; Reck et al., 2009).

These clinical reports support the idea that cortical and STN power and coherence at tremor frequencies increase with the manifestation of tremor, but this phenomenon has not been modeled in rodents. Therefore, the present study characterized the temporal pattern of oral EMG activity and associated changes in LFPs recorded from M1 and STN during the TJMs induced by the non-selective muscarinic agonist pilocarpine (Collins et al., 2010; Collins-Praino et al., 2012; Salamone et al., 2013).

2. Materials and Methods

2.1. Animals

A total of 5 adult male Sprague Dawley rats (Harlan Sprague Dawley, Indianapolis, IN) with no prior drug experience were used in the present experiment. The rats weighed 350-450 g during the course of the experiment and had *ad libitum* access to lab chow and water. Animals

were group-housed prior to surgery in a colony that was maintained at approximately 23°C and had a 12-hour light/dark cycle (lights on at 0700 hrs). Post-surgery, animals were single housed to avoid over grooming around the surgical implant. This study was conducted according to University of Connecticut and NIH guidelines for animal care and use.

2.2 Drug Treatment Procedures and Dose Selection

Pilocarpine was purchased from Sigma Aldrich Chemical (St. Louis, MO) and dissolved in 0.9% saline. The dose of pilocarpine (4.0 mg/kg) was based on previous experiments showing significant induction of jaw movements at this dose (see Collins et al. 2010a for further details).

2.3. Surgical Procedures

Rats were anesthetized with a 1.0 ml/kg IP injection of a cocktail solution containing 10.0 ml of 100mg/mL ketamine plus 0.75 ml of 20.0mg/ml xylazine (Phoenix Scientific, Inc., St. Joseph, MO, USA). Rats were placed in a stereotaxic frame (Kopf, Tujunga, CA, USA), and a midline scalp incision was made. Two electrode arrays consisting of 50µm tungsten wire (California Fine Wire Company, Grover Beach, CA) were bilaterally implanted with a 27-gauge needle approximately 5.0 mm deep into the lateral temporalis muscle (4 EMG electrodes per animal). Previous research has demonstrated that the lateral temporalis muscle is the jaw muscle that shows activity most closely related to TJMs (Cousins et al., 1998). Burr holes were drilled through the skull over the STN (R hemisphere) and M1 (L hemisphere), and two –four electrode arrays were implanted (8 LFP electrodes per animal). LFP electrode arrays were comprised of four linearly spaced 50µm tungsten wires (California Fine Wire Company, Grover Beach, CA). Electrode wire was arranged and separated by fused silica tubing (Polymicro Tubing, Phoenix, AZ), attached to female pins (Omnetics, Minneapolis, MN) and secured in a rectangular five by four pin array. Two stainless steel watch screws driven into the skull above the cerebellum

served as indifferent and ground electrodes. Supplementary anchor screws were positioned as necessary and the entire head-stage ensemble was fortified with dental acrylic. The surgical coordinates, for which bregma and the top of the skull was used as the reference point, were as follows: STN (AP: -3.6, ML: +/- 2.5, DV: -7.5); M1 (AP +1.0, ML +1.9, DV -2.5). Rats recovered for one-week post-surgical procedure.

2.4. Behavioral Measures

Following a one-week recovery period, rats were given an acute IP injection of saline (vehicle). Immediately after vehicle injection, rats were placed into a Plexiglas observation chamber and allowed to habituate for 10 min. At the beginning of this habituation period, the animals were connected to the recording apparatus by a multi-channel tether (Neuralynx, Bozeman, MT) that was attached to a pulley system in the ceiling. Following the habituation period, a trained observer counted tremulous jaw movements for fifteen minutes. TJMs were defined as rapid vertical deflections of the lower jaw that resembled chewing but were not directed at any particular stimulus (Salamone et al. 1998). At the end of the 15-minute observation period, rats were disconnected and returned to their home cages. This procedure was repeated with administration of 4.0mg/kg pilocarpine 24 hours later.

2.5. Electrophysiological Data Acquisition and Analysis

Following the habituation period, wide-band electrical activity was recorded (5050.5 samples/sec) for 15 minutes using a Neuralynx data acquisition system (Bozeman, MT). TJMs were counted simultaneously by a trained observer and noted using event markers through Cheetah data acquisition software (version 5.6.3; Neuralynx, Bozeman, MT). Following data acquisition and during subsequent offline analysis, data were imported into Matlab R2014a (Mathworks, Natick, MA). The raw EMG signal was bandpass filtered between 500 and 1500 Hz

and the Hilbert transform was computed on the bandpass filtered signal. In this regard, the instantaneous (5050.5 samples/sec) EMG envelope amplitude (magnitude of Hilbert transform) was obtained over time. The EMG signal was then full wave rectified and all raw EMG traces presented in the current analysis represent this full wave rectified signal. Event markers were simultaneously imported into Matlab and plotted along with the EMG signal. The presence or absence of these event markers was used to identify TJM and no TJM epochs, respectively. Raw LFP data were imported into Matlab R2014a and down-sampled by a factor of 10 during offline analysis, thus changing the sampling rate to 505.05 samples/s (Hz; 5050.5/10 = 505.05). The raw LFP signal was lowpass filtered to remove high frequency chewing, chattering and/or teeth grinding artifacts (F_c = 200 Hz). Then, the LFP signal was bandpass filtered for tremor (3-7 Hz) and beta frequency (15-30 Hz) and the Hilbert transform was computed on the bandpass filtered signals. Data were examined during: 1) TJM epochs and, 2) No TJM epochs.

All data analysis was conducted using custom written programs in MatLab R2014a (Mathworks, Natick, MA). Power spectral density estimates were obtained using Welch's averaged modified periodogram method (Welch, 1967) during epochs of TJMs and no TJMs. To extract the amplitude modulation (AM) frequency of the EMG signal (e.g., "tremor frequency"; 3-7 Hz), power spectral density estimates were obtained from the envelope (magnitude of Hilbert transform) of the bandpass filtered EMG signal. For LFP data, the power for tremor (3-7 Hz) and beta frequency (15-30 Hz) was calculated from the bandpass filtered signals and represented in units of mV^2. Average power was calculated by taking the sum of the power values within a given frequency range of interest (e.g., 3-7 Hz) and multiplying the sum by the spectral window resolution. Centroid frequency or the weighted mean was calculated by first isolating the frequency range of interest (e.g., 3-7 Hz), indexing the power values within that frequency range

and multiplying them. Then, we divided those values by the sum of the previously indexed power values. Lastly, we took the sum of the aforementioned.

2.6. Statistics

For each of the 5 animals a representative 2.2 second TJM was identified by a trained observer using event markers. The TJM length was determined by the lowest responding animal. Further, within the same recording for each animal a subsequent 2.2 second no TJM time point was isolated as indicated by lack of event markers. For each electrode, the average power and centroid frequency was computed within the frequency range of interest (3-7 Hz and 15-30 Hz) for TJM and no TJM epochs all the while discretized by electrode location (M1 and STN). Paired samples t-tests were computed to asses if there were significant differences in 1) average tremor power during TJMs and no TJMs for M1, 2) average tremor power during TJMs and no TJMs for STN, 3) average beta power during TJMs and no TJMs for M1, 4) average beta power during TJMs and no TJMs for STN, and 5) the same as 1-4, but for centroid frequency. Further, we computed paired-samples t-tests to examine if there were differences in the aforementioned indices as a function of brain area (M1 and STN). Lastly, paired samples t-tests were used to confirm significant differences in number of TJMs per fifteen-minute recording period across vehicle and pilocarpine recordings.

2.7. Histology

At the completion of the experiment, animals were deeply anesthetized with CO_2 and perfused with 0.9% physiological saline followed by 3.7% formaldehyde solution. The brains were extracted and stored in the formaldehyde solution for one week. Then, brains were sliced

(50 µm sections) using a vibratome (Leica, Germany), mounted, Nissl stained using Cresyl Violet and cover-slipped allowing for verification of electrode placements. Photomicrographs of electrode tracks were taken using a Nikon microscope connected to a Spot RT camera system, digitized and prepared for presentation using Adobe Photoshop. Consistent with the histological criteria employed by Brown et al. (2011) only placements that were within 500 µm of the STN, but dorsal to the cerebral peduncles and internal capsule were used for statistical analyses.

3. Results

3.1. Histological verification of electrode placements

A total of 37 LFP electrodes (n= 19 M1 electrodes; n=19 STN electrodes) and 5 EMG electrodes across 5 animals were used in the current analysis. All animals contributed 1 EMG electrode, 3-4 M1 (**Figure 1A**) and 3-4 STN (**Figure 1B**) electrodes. All EMG and LFP data were simultaneously recorded from each animal. M1 electrodes terminated in all cortical layers but were more likely to terminate in deeper layers. Further, most STN electrodes were hits, although a few terminated slightly dorsally or anteriorly (data not shown), but still within the 500 µm criteria put forth by Brown et al. (2011).

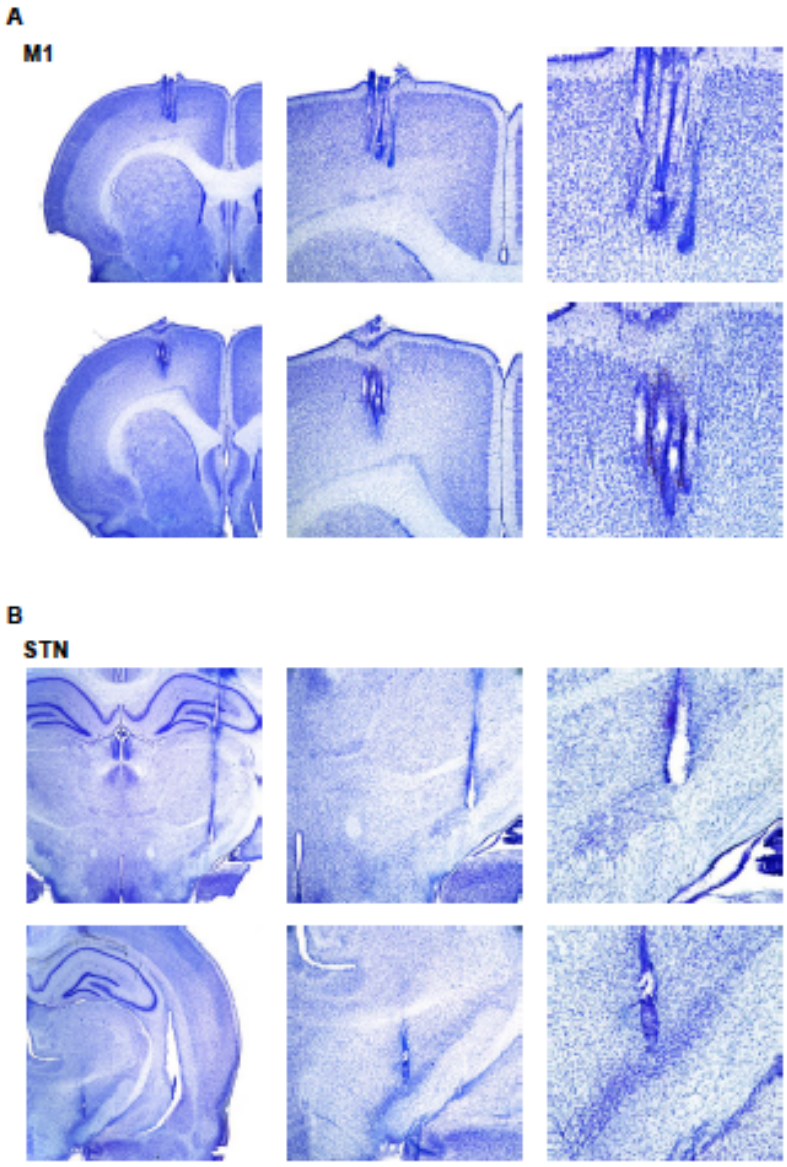

Figure 1: **Verification of electrode placements. A (top)**: Photomicrographs of four representative and simultaneously recorded sites in M1. Middle and right photomicrographs show 4x and 10x close-up of electrode tips, respectively. **A (bottom)**: Same as A (top) but for a different animal. **B (top)**: Photomicrographs of a representative recording site in STN. Middle and right photomicrographs show a 4x and 10x close-up of electrode tips, respectively. **B (bottom)**: Same as B (top) but for a different animal.

3.2. Pilocarpine induces TJMs in the tremor frequency range (3-7 Hz) as reflected by EMG

Administration of pilocarpine significantly induced TJMs compared to vehicle control (Pilo mean: 603.6 $\pm$ 314.4; Veh mean: 14.4 $\pm$ 9.8; t(4) = 4.3, p <. 05). Although vehicle

conditions were used to verify the ability of pilocarpine to produce TJMs, large behavioral differences existed between vehicle and pilocarpine recordings that made electrophysiological comparisons between these two signals unsuitable (i.e., no tremor bursts, but more movement artifact, under vehicle conditions). Because of these differences, all EMG and LFP data analysis were conducted on epochs of TJMs and no TJMs within the pilocarpine recording for each animal.

During bouts of jaw movement activity, the bandpass filtered (500-1500 Hz) and full wave rectified EMG signal was marked by rhythmic activity in the 3-7 Hz range (**Figure 2A top, left; red**). Conversely, during periods of quiescence, no rhythmic activity was observed in the EMG (**Figure 2A bottom, left; blue**). Spectrograms indicated the same pattern of activity as the filtered EMG traces (**Figure 2A, right**). For the traces presented in **Figure 2A**, power spectral analysis revealed strong rhythmicity in the envelope of the EMG signal with a fundamental frequency of 4 Hz along with robust 2^{nd} and 3^{rd} harmonics (**Figure 2B, red**). Epochs of quiescence failed to exhibit amplitude modulation of the EMG signal within the tremor frequency range (**Figure 2B, blue**) and, show relatively little power overall. Upon examination of the entire pilocarpine recording for the same representative animal, rodents continued to exhibit dominant power of the EMG envelope within the tremor frequency range, although the harmonics were largely attenuated (**Figure 2C**). Importantly, this animal exhibited TJMs for 23.15% (3.47/15 minutes) of the recording session (**Figure 2C right)** indicating the robustness of the observed phenomenon.

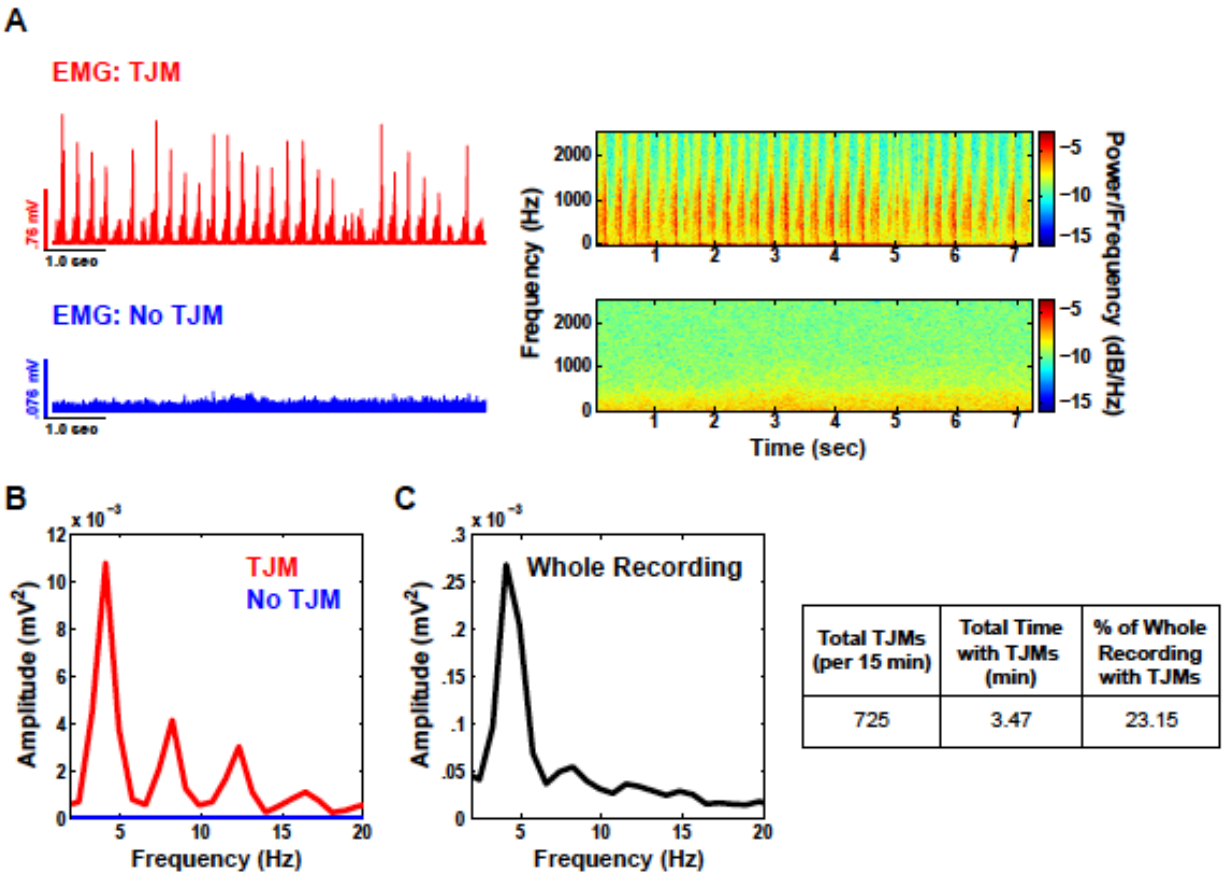

Total TJMs (per 15 min)	Total Time with TJMs (min)	% of Whole Recording with TJMs
725	3.47	23.15

Figure 2: **Pilocarpine induces TJMs in the tremor frequency range as reflected by EMG activity. A (top)**: EMG electrode trace bandpass filtered for EMG frequency (500-1500 Hz) and full wave rectified during a long epoch of TJMs (red; 7.3 seconds) for a representative animal. The spectrogram indicates the same pattern of rhythmic activity as the EMG trace. **A (bottom)**: Same animal and recording as presented in A, but for a long period of quiescence (blue; 7.3 seconds). The spectrogram indicates little rhythmic activity during bouts lacking TJMs. **B**: Power spectrum of the EMG envelope for the same traces as presented in A. As can be seen, there is clear 3-7 Hz rhythmicity and strong harmonics during TJM epochs, which is absent during periods of quiescence. **C (left)**: Power spectrum of the entire pilocarpine recording (sans TJM and no TJM epoch isolation) for the same animal as presented in A and B. **C (right)**: Behavior of the same animal as presented previously across the entirety of pilocarpine recording.

3.3. Power in the tremor frequency band increases during TJMs in M1 and STN

Upon examination of simultaneously recorded M1 LFPs for the same animal as in **Figure 2**, the raw (**Figure 3A top**) and bandpass filtered (3-7 Hz; **Figure 3A middle**) LFP signals revealed increased power in the tremor frequency band during epochs of TJMs (**Figure 3A left, red**), but not during bouts of quiescence (**Figure 3A right, blue**). The LFP signal was indexed

during epochs of TJMs and no TJMs as indicated by EMG event markers or lack thereof, respectively. Spectrograms of the raw signal revealed differential patterns of LFP activity for bouts of TJMs and quiescence (**Figure 3A bottom**). The power spectrum of the raw LFP signal filtered for tremor frequencies (3-7 Hz) during epochs of TJMs (red) and no TJMs (blue) indicated strong LFP power in the tremor range with a peak at ~4 Hz for bouts of TJMs, while little LFP power existed at such frequencies for bouts lacking TJMs. At a simultaneously recorded STN site, the same pattern of activity was present (**Figure 3B**). Overall, the bandpass filtered LFP signal (3-7 Hz) during bouts of TJMs and the subsequent power spectrum of that signal revealed strong power in the 3-7 Hz range, whereas bouts of quiescence did not exhibit this effect (**Figure 3B**).

Summary data from all animals revealed the same pattern of effects. Overall, M1 LFPs during TJM epochs (red) exhibited significantly more power in the 3-7 Hz range as compared to no TJM (blue) epochs (**Figure 3C**; $t(18) = 5.13$, $p < .05$). The same pattern of activity existed for STN recording sites (**Figure 3C, right**; $t(18) = 4.55$, $p < .05$). Further, M1 exhibited more power in the tremor band during TJM and no TJM epochs compared to STN (TJM: $t(18) = 3.47$, $p < .05$; no TJM: $t(18) = 3.26$, $p < .05$). Analysis of centroid frequency (**Figure 3D**) revealed no differences between bouts of TJMs and no TJMs within a given brain area (e.g., M1 TJM vs. M1 no TJM; M1: $t(18) = -0.79$, $p > .05$; STN: $t(18) = -0.36$, $p > .05$). Moreover, there were no significant differences in LFP centroid frequency between TJM and no TJM epochs across brain areas (e.g., M1 TJM vs. STN TJM; TJM: $t(18) = 0.51$, $p > .05$; No TJM: $t(18) = 1.88$, $p > .05$).

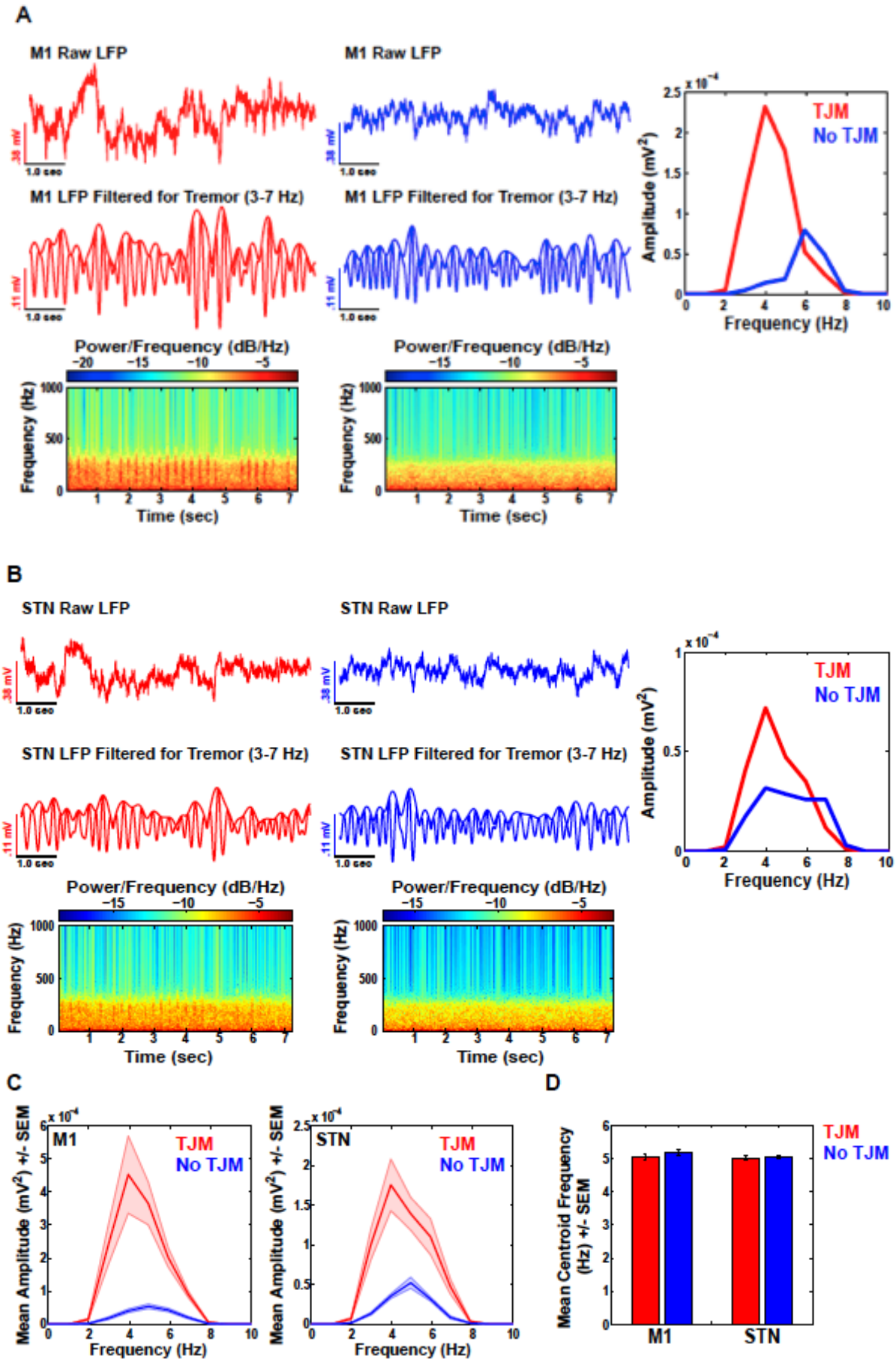
A
M1 Raw LFP
M1 Raw LFP
M1 LFP Filtered for Tremor (3-7 Hz)
M1 LFP Filtered for Tremor (3-7 Hz)
Power/Frequency (dB/Hz)
Power/Frequency (dB/Hz)
Frequency (Hz)
Time (sec)
Amplitude (mV²)
Frequency (Hz)
TJM
No TJM
B
STN Raw LFP
STN Raw LFP
STN LFP Filtered for Tremor (3-7 Hz)
STN LFP Filtered for Tremor (3-7 Hz)
C
M1
STN
Mean Amplitude (mV²) +/- SEM
D
Mean Centroid Frequency (Hz) +/- SEM

Figure 3: **Power in tremor frequency band increases during TJMs in M1 and STN. A**: Raw (top) and bandpass filtered (3-7 Hz; middle) M1 LFP traces during epochs of TJMs (red) and no TJMs (blue) for the same representative animal presented in Figure 2. **A (bottom)**: Corresponding spectrograms for the raw M1 signal presented in the top panel of A during TJM and no TJM epochs. Overall, the spectrograms indicate rhythmicity in the LFP during periods of TJMs that is lacking during periods of quiescence. **A (right)**: Power spectrum of the bandpass filtered LFP signal presented in the middle panel of A during the TJM and no TJM epoch. Tremor frequency power increases substantially during periods of TJMs, while little tremor power exists during epochs of quiescence. **B**: Same as A, but for a simultaneously recorded STN site for the same representative animal presented in panel A. **C**: Summary data for tremor frequency power across all animals for TJM and no TJM epochs for M1 and STN. As can be seen, tremor band power dominates during the presence of TJMs, but not for bouts lacking TJMs. **D**: Summary data across all animals for tremor band centroid frequency as a function of TJM and no TJM epochs for M1 and STN recording sites. Overall, there were no differences in centroid frequency across behavioral state or brain area.

3.4. Beta band power does not increase during TJMs in M1 and STN

Simultaneously recorded M1 LFPs for the animal shown in **Figure 2 and 3**, revealed similar LFP beta band power during epochs of TJMs (**Figure 4A left, red**) and epochs of quiescence (**Figure 4A right, blue**) for the raw (**Figure 4A top**) and bandpass filtered (15-30 Hz; **Figure 4A middle**) LFP signals. Importantly, the data shown here are for the same time points as presented in **Figure 2 and 3**, but here data were filtered for beta (15-30 Hz) instead of tremor frequencies (3-7 Hz). A closer look at the signal revealed similar instantaneous fluctuations in the LFP during active (**Figure 4A bottom, left**) and quiet (**Figure 4A bottom, right**) bouts. The power spectrum of the raw LFP signal filtered for beta band activity during epochs of TJMs (red) and no TJMs (blue) revealed strong LFP beta band power, but no alterations in power across behavioral state (e.g., bouts of TJMs vs. no TJMs). At a simultaneously recorded STN site, the same pattern of activity was present (**Figure 4B**). Overall, the bandpass filtered LFP signal (15-30 Hz) and subsequent power spectrum of that

signal during epochs of TJMs and quiescence revealed no differences in beta band power (**Figure 4B**).

Summary data from all animals demonstrate the same trend as represented in **Figure 4A/B**. Overall, M1 LFPs during TJM epochs (red) and no TJM epochs (blue) exhibited similar levels of beta band power (**Figure 4C**; t(18) = 1.48, $p > .05$). For STN, the same pattern of activity existed (**Figure 4C, right**; t(18) = 0.65, $p > .05$). Further, M1 exhibited higher beta band power during epochs of TJMs and no TJMs as compared to STN (TJM: t(18) = 2.76, $p < .05$; no TJM: t(18) = 3.12, $p < .05$). Moreover, TJM epochs exhibited lower centroid beta band frequency compared to no TJM epochs for both M1 and STN (**Figure** 4D; M1: t(18) = -2.84, $p < .05$; STN: t(18) = -3.57, $p < .05$, respectively). Further, beta band frequency was higher in M1 during TJM epochs compared to STN (t(18) = 3.63, $p < .05$). Alternatively, there was no difference in beta band frequency between M1 and STN during periods of quiescence (t(18) = -0.47, $p > .05$).

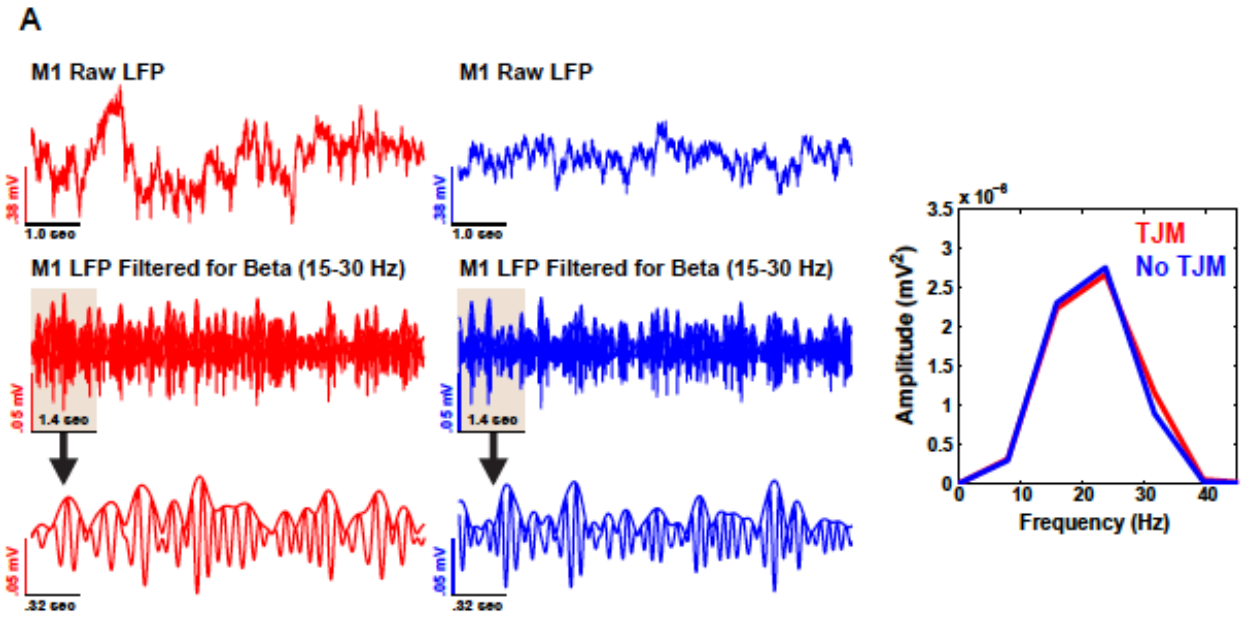

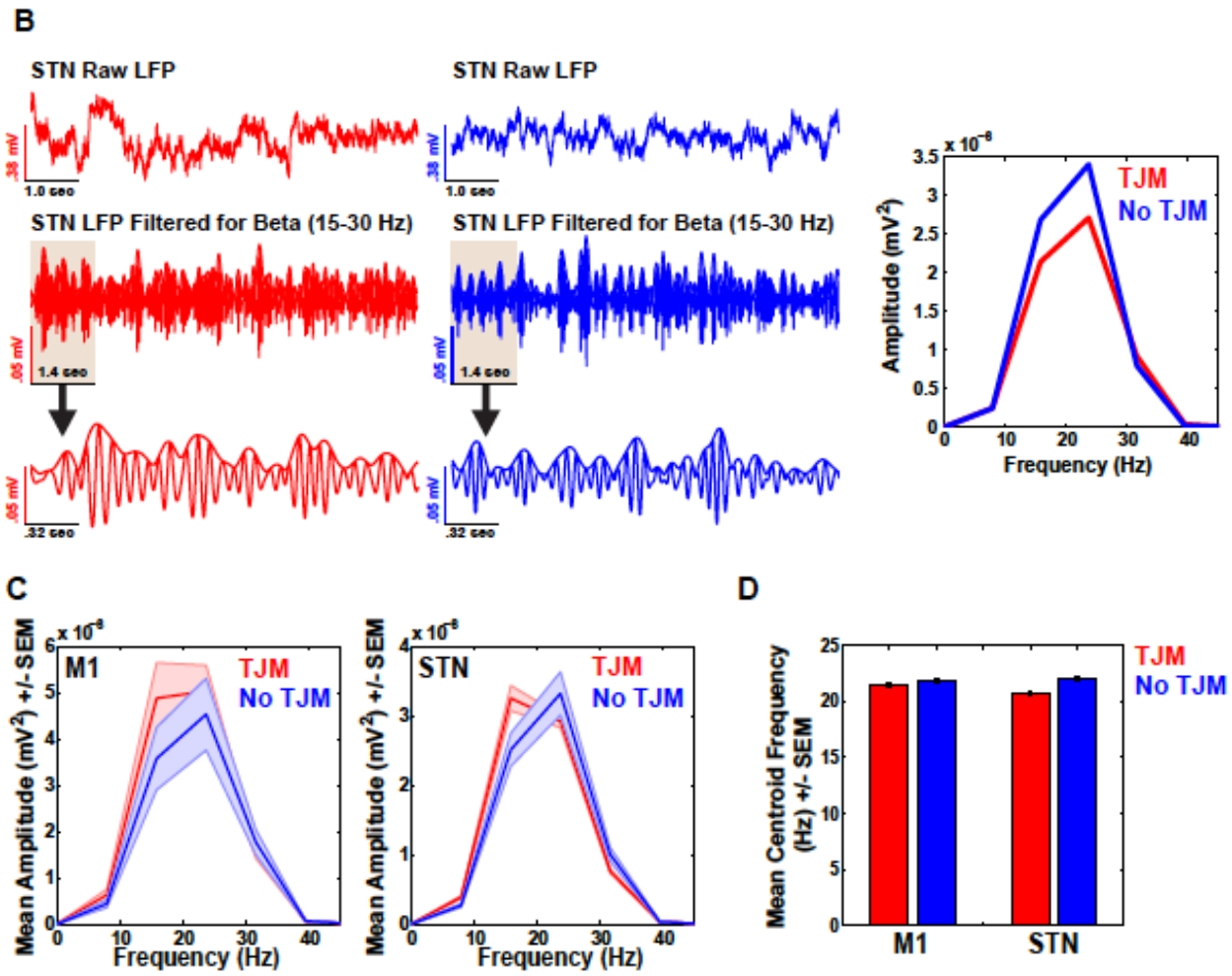

Figure 4: **Beta band power does not increase during TJMs in M1 and STN. A**: Raw (top) and bandpass filtered (15-30 Hz; middle) M1 LFP traces during epochs of TJMs (red) and no TJMs (blue) for the same representative animal presented in Figure 2 and 3. **A (bottom)**: The first 1.4 seconds of the middle panel of A to show instantaneous LFP fluctuations. **A (right)**: Power spectrum of the bandpass filtered LFP signal presented in the middle panel of A during the TJM and no TJM epoch. Beta frequency power does not increase during periods of TJMs, while little **B**: Same as A, but for a simultaneously recorded STN site for the same representative animal presented in panel A. **C**: Summary data for beta band power across all animals for TJM and no TJM epochs for M1 and STN. As can be seen, beta band power is similar during across behavioral states. **D**: Summary data across all animals for beta band centroid frequency as a function of TJM and no TJM epochs for M1 and STN recording sites.

4. Discussion

Previous research has shown that the non-selective muscarinic agonist pilocarpine is a tremorogenic agent. Pilocarpine induces a robust TJM response in the 3-7 Hz frequency range that is reduced by antiparkinsonian agents (Salamone et al., 2005; Betz et al., 2007; Collins et al.,

2010; Podurgiel et al., 2013a), conditional neural knockout of adenosine A_{2A} receptors (Salamone et al., 2013), and deep brain stimulation of the STN (Collins-Praino et al., 2012). Evidence indicates that the TJMs induced by pilocarpine are due to stimulation of M2 or M4 muscarinic receptors in the ventrolateral neostriatum of the rat, which is the homologue of the ventral putamen of primates (Salamone et al., 1990, 1998; Mayorga et al., 1997, 1999). For these reasons, pilocarpine was selected for the present studies in order to induce a robust oral tremor that would allow for the assessment of tremor-related cortical and subthalamic LFP activity.

Network activation as measured by LFP activity in M1 and STN can be used as a tool to better understand transient dynamics across distributed neural networks. Similar to analysis of variations in the blood-oxygen-dependent signal used in functional neuroimaging (Logothetis and Wandell, 2004; Law et al., 2005), detailed analysis of mesoscopic signals such as the LFP and EEG reveal the engagement of distributed neural circuits in relation to tremorogenesis— a cardinal symptom of Parkinsonism. Abnormalities in long-range connectivity between brain areas have been postulated as an important pathophysiological mechanism underlying brain dysfunctions (Hutchison et al., 2004; Mallet et al., 2008). However, it remains unclear how perturbed connectivity relates to motor symptoms such as tremorogenesis, and how it is manifested in the dynamic interactions of neuronal circuits.

In the present study, we simultaneously recorded LFPs from the primary motor cortex and subthalamic nucleus as well as EMG from the lateral temporalis muscle in a rat model of drug-induced tremor. The temporalis was chosen because of previous research indicating that activity of this jaw closing muscle is a critical marker of observable TJM activity (Cousins et al., 1998). The present results indicate that administration of the muscarinic agonist pilocarpine induces TJMs in rats that fall into the frequency range associated with Parkinsonian resting

tremor (3-7 Hz), with a peak frequency of approximately 4 Hz, and harmonics at higher frequencies. These data are consistent with previous studies indicating that cholinomimetic drugs, including muscarinic agonists and anticholinesterases, can induce or exacerbate resting tremor. Administration of the anticholinesterase physostigmine to PD patients was reported to exacerbate parkinsonian symptoms, including tremor, and these motor deficits were attenuated by coadministration of centrally-acting muscarinic antagonists (Duvoisin 1967). For many decades, non-selective muscarinic receptor antagonists have been used to treat idiopathic and drug-induced Parkinsonism (McEvoy, 1983). Anticholinesterases are prescribed to treat the cognitive deficits associated with Alzheimer's Disease (see Birks, 2006 for review), and these drugs have been shown to induce Parkinsonian symptoms, including tremor, as side effects (Ott and Lannon, 1992; Arai, 2000; Aarsland et al., 2003; Grace et al., 2009). In animal studies, muscarinic agonists such as tremorine and oxotremorine have been widely recognized to act as tremorogenic agents (Brimblecombe, 1975). Furthermore, muscarinic agonists and anticholinesterases induce TJMs in rodents, and co-administration of antiparkinsonian agents including DA agonists, muscarinic antagonists, and adenosine A_{2A} antagonists have been shown to reduce cholinomimetic-induced TJMs (Salamone et al. 1986; Baskin et al., 1994; Mayorga et al., 1997; Salamone et al., 1998; Simola et al., 2004, 2006; Miwa et al., 2009; Collins et al., 2010a, 2011).

The induction of TJMs by pilocarpine was associated with strong rhythmicity in the envelope of the EMG signal with a peak frequency of approximately 4 Hz along with robust second and third harmonics, which is consistent with EMG recordings from the forearms of PD patients during periods of tremor (Liu et al., 2002; Timmerman et al., 2003; Wang et al., 2005; Reck et al., 2009; Hirschmann et al., 2013). This EMG activity was accompanied by an increase

in power at tremor frequency (3-7 Hz) in M1 and the STN. In PD patients, pathological oscillatory neuronal activity in the open and closed loop connections between the cortex, basal ganglia, and thalamus is thought to underlie tremorogenesis (Hutchison et al., 2004). Simultaneously recorded magnetoencephalography and forearm EMG in PD patients has allowed researchers to characterize the cortical regions that are coherent with muscle activity during periods of resting tremor (Oswal et al., 2013). These studies indicate a strong coherence between EMG of forearm muscles and M1 activity at tremor frequency and its second harmonic (Timmerman et al., 2003).

Oscillatory activity in the STN of PD patients has been well characterized, as researchers are able to record LFPs from patients undergoing implantation of stimulating electrodes for deep brain stimulation. In recent years, the primary focus has been on increased oscillatory activity in the beta band (~15-30 Hz), since there is evidence that increased beta power in the STN is associated with motor control, particularly akinesia-rigidity (Brown et al., 2001; Levy et al., 2002; Priori et al., 2004; Brown and Williams, 2005; Kuhn et al., 2006). Conversely, resting tremor has not been shown to correlate with beta band activity in the STN of PD patients (Kuhn et al., 2005). Instead, the development of tremor has been associated with the emergence of oscillations in the tremor frequency range (3-7 Hz) as indicated by power spectra of STN LFPs, and coherence between STN LFPs and EMG activity at tremor frequency (Brown et al., 2001; Levy et al., 2000; Liu et al., 2002; Wang et al., 2005; Reck et al., 2009; Hirschmann et al., 2013). In a recent study by Hirschmann et al. (2013) the emergence of tremor in PD patients was shown to be associated with an increase of cerebral synchronization at tremor frequency and second harmonic in a network that includes both STN and M1. Additionally, in African green monkeys treated with 1-methyl-4-phenyl-1,2,3,6-tetrahydropyridine (MPTP), the development of resting

tremor was associated with the emergence of oscillations at tremor frequency in the STN (Bergman et al., 1994). Results from our experiment are line with the findings reported in the clinical and non-human primate studies, as we saw increased power in M1 and STN in the tremor, but not beta frequency range during periods of TJMs. Moreover, the present results are consistent with previous studies demonstrating that the STN is a critical part of the basal ganglia circuitry that is involved in motor dysfunctions related to Parkinsonism. Lesions or inactivation of STN have been shown to reverse motor dysfunctions in rodent models (Centonze et al., 2005; Baunez and Gubellini 2010). In addition, high frequency stimulation of STN has been reported to restore motor function in rodent models of Parkinsonism (Baunez 2011; Brown et al., 2011), and to attenuate drug-induced TJMs in rats (Collins-Praino et al., 2011).

To date, this phenomenon has been well documented in the clinical literature, but very little has been done to study these oscillatory alterations in rodent models. It has, however, been shown that LFPs recorded from the frontal cortex and STN of rats with 6-hydroxydopamine lesions of midbrain dopaminergic neurons show increased power and coherence in the beta frequency band (Sharott et al., 2005; Mallet et al., 2008). It should be noted that these studies were using a model that involved neurotoxic depletion of DA, whereas our study employed a model of drug-induced Parkinsonian resting tremor. In the present study, though the rats appeared to have reduced locomotion after pilocarpine administration, they were not completely akinetic, and occasionally moved about the chamber during recording. Therefore, our study specifically evaluated the physiological correlates of tremor by using an agent that induces a robust tremorogenic (i.e., TJM) response. By providing physiological and behavioral correlates of tremor, this model could be utilized in preclinical studies focused on the development of Parkinsonian treatments that specifically target tremor.

References

Aarsland D, Hutchison M, and Larsen JP (2003) Cognitive, psychiatric and motor response to galantamine in Parkinson's disease with dementia. Int J Geriat Psychiat 18:937-941.

Arai, M (2000). Parkinsonism onset in a patient concurrently using tiapride and donepezil. Intern Med, 39:863.

Baskin P, Salamone JD (1993) Vacuous jaw movements in rats induced by acute reserpine administration: interactions with different doses of apomorphine. Pharmacol Biochem Behavior 46: 793-797.

Baskin PP, Gianutsos G, Salamone JD (1994) Repeated scopolamine injections sensitize rats to pilocarpine-induced vacuous jaw movements and enhance striatal muscarinic receptor binding. Pharmacol Biochem Behav 49(2):437-42.

Baunez C (2011) A few examples of the contribution of animal research in rodents for clinical application of deep brain stimulation. Prog Brain Res 194:105-116.

Baunez C, Gubellini P (2010) Effects of GPi and STN inactivation on physiological, motor, cognitive and motivational processes in animal models of Parkinson's disease. Prog Brain Res 183: 235-58.

Bergman H, Wichmann T, Karmon B, DeLong MR (1994). The primate subthalamic nucleus. II.

Neuronal activity in the MPTP model of parkinsonism. J Neurophysiol., 72(2):507-20.

Betz AJ, McLaughlin PJ, Burgos M, Weber SM and Salamone JD (2007) The muscarinic receptor antagonist tropicamide suppresses tremulous jaw movements in a rodent model of parkinsonian tremor: possible role of M4 receptors. Psychopharmacology 194:347-359.

Birks J (2006) Cholinesterase inhibitors for Alzheimer's disease. Cochrane Database Syst Rev 1:CD005593.

Brimblecombe RW (1975) Review of tremorogenic agents. In: Cholinergic Mechanisms (Walter PG, ed), pp405-10. New York: Raven Press.

Brown P, Oliviero A, Mazzone P, Insola A, Tonali P, Di Lazzaro V (2001) Dopamine dependency of oscillations between subthalamic nucleus and pallidum in Parkinson's disease. J Neurosci 1;21(3):1033-8.

Brown P (2003) Oscillatory nature of human basal ganglia activity: relationship to the pathophysiology of Parkinson's disease. Mov Disord 18(4):357-63.

Brown P, Williams D (2005) Basal ganglia local field potential activity: character and functional significance in the human. Clin Neurophysiol 116(11):2510-9.

Brown AR, Antle MC, Hu B, Teskey GC (2011) High frequency stimulation of the subthalamic nucleus acutely rescues motor deficits and neocortical movement representations following 6-hydroxydopamine administration in rats. Exp Neurol 231:82-90.

Buzsáki G, Chrobak JJ (1995) Temporal structure in spatially organized neuronal ensembles: a role for interneuronal networks. Curr Opin Neurobiol 5:504-10.

Centonze D, Gubellini P, Rossi S, Picconi B, Pisani A, Bernardi G, Calabresi P, Baunez C (2005) Subthalamic nucleus lesion reverses motor abnormalities and striatal glutamatergic overactivity in experimental parkinsonism. Neuroscience 133(3):831-40.

Collins LE, Galtieri DJ, Brennum LT, Sager TN, Hockemeyer J, Müller CE, Hinman JR, Chrobak JJ, Salamone JD (2010) Cholinomimetic-induced tremulous jaw movements are suppressed by the adenosine A2A antagonists MSX-3 and SCH58261, but not the adenosine A1 antagonist DPCPX: Possible relevance for drug-induced parkinsonism. Pharmacol Biochem Behav 94: 561-569.

Collins-Praino LE, Paul NE, Rychalsky KL, Hinman JR, Chrobak JJ, Senatus PB, Salamone JD (2011) Pharmacological and physiological characterization of the tremulous jaw movement model of parkinsonian tremor: potential insights into the pathophysiology of tremor. Front Syst Neurosci 5:49.

Collins-Praino LE, Paul NE, Ledgard F, Podurgiel SJ, Kovner R, Baqi Y, Müller CE, Senatus

PB, Salamone JD (2012) Deep brain stimulation of the subthalamic nucleus reverses oral tremor in pharmacological models of parkinsonism: interaction with the effects of adenosine A2A antagonism. Eur J Neurosci 38(1):2183-91.

Correa M, Wisniecki A, Betz A, Dobson DR, O'Neill MF, O'Neill MJ, Salamone JD (2004) The adenosine A2A antagonist KF 17837 reverses the locomotion suppression and tremulous jaw movements induced by haloperidol in rats: Possible relevance to parkinsonism. Behav Brain Res 148: 47-54.

Cousins MS, Carriero DL, Salamone JD (1997) Tremulous jaw movements induced by the acetylcholinesterase inhibitor tacrine: Effects of antiparkinsonian drugs. Eur J Pharmacol 322:137-145.

Cousins MS, Atherton A, Salamone JD (1998) Behavioral and electromyographic characterization of the local frequency of tacrine-induced tremulous jaw movements. Physiol Behav 64:153-158.

Czeutzfeldt OD, Watanabe S, Lux HD (1966) Relations between EEG phenomena and potentials of single cortical cells II. Spontaneous and convulsoid activity. ElectroenchephClin Neurophysiol 20: 19-37.

Deuschl G, Raethjen J, Baron R, Lindemann M, Wilms H, Krack P (2000) The pathophysiology of parkinsonian tremor: a review. J Neurol 247: V33-V48.

Duvoisin RC (1967) Cholinergic-anticholinergic antagonism in parkinsonism. Arch Neurol 17:124-136.

Findley LJ, Gresty MA (1981) Tremor. Brit J Hosp Med 26: 16-32.

George JS, Strunk J, Mak-McCully R, Houser M, Poizner H, Aron AR (2013) Dopaminergic therapy in Parkinson's disease decreases cortical beta band coherence in the resting state and increases cortical beta band power during executive control. Neuroimage Clin 3:261-70.

Grace J, Amick MM, Friedman JH (2009) A double blind comparison of galantamine hydrobromide ER and placebo in Parkinson disease. J Neurol Neurosurg Psychiat 80(1):18–23.

Hammond C, Bergman H, Brown P (2007) Pathological synchronization in Parkinson's disease: networks, models and treatments. Trends Neurosci 30(7):357-64.

Hirschmann J, Hartmann CJ, Butz M, Hoogenboom N, Ozkurt TE, Elben S, Vesper J, Wojtecki L, Schnitzler A (2013) A direct relationship between oscillatory subthalamic nucleus-cortex coupling and rest tremor in Parkinson's disease. Brain 136(Pt 12):3659-70.

Hornykiewicz, O (1973) Dopamine in the basal ganglia. Its role and therapeutic implications including the clinical use of L-DOPA. British Medical Bulletin 29 *2 172-178.

Hutchison WD, Dostrovsky JO, Walters JR, Courtemanche R, Boraud T, Goldberg J, Brown P (2004) Neuronal oscillations in the basal ganglia and movement disorders: evidence from whole animal and human recordings. J Neurosci 24(42):9240-3.

Jicha G and Salamone JD (1991) Vacuous jaw movements and feeding deficits in rats with ventrolateral striatal dopamine depletions: possible model of parkinsonian symptoms. J Neurosci 11:3822-3829.

Kühn AA, Trottenberg T, Kivi A, Kupsch A, Schneider GH, Brown P (2005) The relationship between local field potential and neuronal discharge in the subthalamic nucleus of patients with Parkinson's disease. Exp Neurol 194(1):212-20.

Kühn AA, Kupsch A, Schneider GH, Brown P (2006) Reduction in subthalamic 8-35 Hz oscillatory activity correlates with clinical improvement in Parkinson's disease. Eur J Neurosci 23(7):1956-60.

Law JR, Flanery MA, Wirth S, Yanike M, Smith AC, et al. (2005) Functional magnetic resonance imaging activity during the gradual acquisition and expression of paired-associate memory. J Neurosci 25:5720-5729.

Levy R, Hutchison WD, Lozano AM, Dostrovsky JO (2000) High-frequency synchronization of

neuronal activity in the subthalamic nucleus of parkinsonian patients with limb tremor. J Neurosci 20(20):7766-75.

Levy R, Ashby P, Hutchison WD, Lang AE, Lozano AM, Dostrovsky JO (2002) Dependence of subthalamic nucleus oscillations on movement and dopamine in Parkinson's disease. Brain 125(Pt 6):1196-209.

Liu X, Ford-Dunn HL, Hayward GN, Nandi D, Miall RC, Aziz TZ, Stein JF (2002) The oscillatory activity in the Parkinsonian subthalamic nucleus investigated using the macro-electrodes for deep brain stimulation. Clin Neurophysiol 113(11):1667-72.

Logothetis NK, Wandell BA (2004) Interpreting the BOLD signal. Annu Rev Physiol 66:735-769.

Mallet N, Pogosyan A, Sharott A, Csicsvari J, Bolam JP, Brown P, Magill PJ (2008) Disrupted dopamine transmission and the emergence of exaggerated beta oscillations in subthalamic nucleus and cerebral cortex. J Neurosci 28(18):4795-806.

Marsden C, Duvoisin R, Jenner P, Parkes J, Pycock C, Tarsy, D (1975) Relationship between animal models and clinical parkinsonism. Advances in Neurology 9:165-175.

Mayorga AJ, Carriero DL, Cousins MS, Gianutsos G, Salamone JD (1997) Tremulous jaw movements produced by acute tacrine administration: possible relation to parkinsonian side effects. Pharmacol Biochem Behav 56:73-279.

Mayorga AJ, Cousins MS, Conlan A, Gianutsos G, Salamone JD (1999) Characterization of the muscarinic receptor subtype mediating pilocarpine-induced tremulous jaw movements in rats. Eur J Pharmacol 364:7-11.

McEvoy JP (1983) The clinical use of anticholinergic drugs as treatments for extrapyramidal side effects of neuroleptic drugs. J Clin Psychpharmacol 3:288-302.

Miwa H, Kubo T, Suzuki A, Kondo T (2009) Effects of zonisamide on c-Fos expression under conditions of tacrine-induced tremulous jaw movements in rats: a potential mechanism underlying its anti-parkinsonian tremor effect. Parkinsonism Relat Disord 15: 30-35.

Oswal A, Brown P, Litvak V (2013) Synchronized neural oscillations and the pathophysiology of Parkinson's disease. Curr Opin Neurol 26(6):662-70.

Ott BR, Lannon MC (1992) Exacerbation of Parkinsonism by tacrine. Clin Neuropharm 15:322-325.

Podurgiel S, Collins-Praino LE, Yohn S, Randall PA, Roach A, Lobianco C, Salamone JD (2013a) Tremorolytic effects of safinamide in animal models of drug-induced parkinsonian tremor. Pharmacol Biochem Behav 105:105-11.

Podurgiel SJ, Nunes EJ, Yohn SE, Barber J, Thompson A, Milligan M, Lee CA, López-Cruz L, Pardo M, Valverde O, Lendent C, Baqi Y, Müller CE, Correa M, Salamone JD (2013b) The vesicular monoamine transporter (VMAT-2) inhibitor tetrabenazine induces tremulous jaw movements in rodents: implications for pharmacological models of parkinsonian tremor. Neuroscience 250:507-519.

Podurgiel SJ, Milligan MN, Yohn SE, Purcell LJ, Contreras-Mora HM, Correa M, Salamone JD (2015) Administration Exacerbates Oral Tremor and Striatal Dopamine Depletion in a Rodent Pharmacological Model of Parkinsonism. Neuropsychopharmacology, Epub ahead of print.

Priori A, Foffani G, Pesenti A, Tamma F, Bianchi AM, Pellegrini M, Locatelli M, Moxon KA, Villani RM (2004) Rhythm-specific pharmacological modulation of subthalamic activity in Parkinson's disease. Exp Neurol 189(2):369-79.

Reck C, Florin E, Wojtecki L, Krause H, Groiss S, Voges J, Maarouf M, Sturm V, Schnitzler A, Timmermann L (2009) Characterisation of tremor-associated local field potentials in the subthalamic nucleus in Parkinson's disease. Eur J Neurosci 29(3):599-612.

Salamone JD, Lalies MD, Channell SL, Iversen SD (1986) Behavioural and pharmacological characterization of the mouth movements induced by muscarinic agonists in the rat. Psychopharmacology (Berl) 88(4):467-71.

Salamone JD, Johnson CJ, McCullough LD, Steinpreis RE (1990) Lateral striatal cholinergic mechanisms involved in oral motor activities in the rat. Psychopharmacology 102: 529-534.

Salamone JD, Baskin P (1996) Vacuous jaw movements induced by acute reserpine and low-dose apomorphine: possible model of parkinsonian tremor. Pharmacol Biochem Behav 53: 179-183.

Salamone JD, Mayorga AJ, Trevitt JT, Cousins MS, Conlan A, Nawab A (1998) Tremulous jaw movements in rats: a model of parkinsonian tremor. Prog Neurobiol 56:591-611.

Salamone JD, Carlson BB, Rios C, Lentini E, Correa M, Wisniecki A, Betz A (2005) Dopamine agonists suppress cholinomimetic-induced tremulous jaw movements in an animal model of Parkinsonism: tremorolytic effects of pergolide, ropinirole and CY 208-243. Behav Brain Res 156:173-179.

Salamone JD, Betz AJ, Ishiwari K, Felsted J, Madson L, Mirante B, Clark K, Font L, Korbey S, Sager TN, Hockemeyer J, Muller CE (2008a) Tremorolytic effects of adenosine A2A antagonists: implications for parkinsonism. Front Biosci 13:3594-3605.

Salamone JD, Ishiwari K, Betz AJ, Farrar AM, Mingote SM, Font L, Hockemeyer J, Müller CE, Correa M (2008b) Dopamine/adenosine interactions related to locomotion and tremor in animal models: Possible relevance to parkinsonism. Parkinsonism Relat Disord 14:S130-S134.

Salamone JD, Collins-Praino LE, Pardo M, Podurgiel SJ, Baqi Y, Mu□ller CE, Schwarzschild MA, Correa M (2013) Conditional neural knockout of the adenosine A2A receptor and pharmacological A2A antagonism reduce pilocarpine-induced tremulous jaw movements: Studies with a mouse model of parkinsonian tremor. Eur Neuropsychopharmacol 23(8):972-7.

Sharott A, Magill PJ, Harnack D, Kupsch A, Meissner W, Brown P (2005) Dopamine depletion increases the power and coherence of beta-oscillations in the cerebral cortex and subthalamic nucleus of the awake rat. Eur J Neurosci 21(5):1413-22.

Simola N, Fenu S, Baraldi PG, Tabrizi MA, Morelli M (2004) Blockade of adenosine A2A receptors antagonizes parkinsonian tremor in the rat tacrine model by an action on specific striatal regions. Exp Neurol 189:182-188.

Simola N, Fenu S, Baraldi PG, Tabrizi MA, Morelli M (2006) Dopamine and adenosine receptor interaction as basis for the treatment of Parkinson's disease. J Neurol Sci 248:48-52.

Timmermann L, Gross J, Dirks M, Volkmann J, Freund HJ, Schnitzler A (2003) The cerebral oscillatory network of parkinsonian resting tremor. Brain 126(Pt 1):199-212.

Wang SY, Aziz TZ, Stein JF, Liu X (2005) Time-frequency analysis of transient neuromuscular

events: dynamic changes in activity of the subthalamic nucleus and forearm muscles related to the intermittent resting tremor. J Neurosci Methods 145(1-2):151-8.

Welch PD (1967). The use of fast fourier transform for the estimation of power spectra: a method based on time averaging over short, modified periodograms. IEEE Trans Audio Electroacoust 15: 70–73.